Journal of Photochemistry and Photobiology A: Chemistry 207 (2009) 288–296

Contents lists available at ScienceDirect

Journal of Photochemistry and Photobiology A: Chemistry

journal homepage: www.elsevier.com/locate/jphotochem

Aggregation behavior of aqueous tetrakis(4-sulfonatophenyl)porphyrin in the presence of 1-butyl-3-methylimidazolium tetrafluoroborate

Maroof Ali, Siddharth Pandey*

Department of Chemistry, Indian Institute of Technology Delhi, Hauz Khas, New Delhi 110016, India

ARTICLE INFO

Article history:
Received 8 June 2009
Received in revised form 18 July 2009
Accepted 27 July 2009
Available online 3 August 2009

Keywords:
Porphyrin
Ionic liquid
J-aggregate
Kinetics
Fluorescence
Aggregation

ABSTRACT

Due to their unusual properties the role of ionic liquids (ILs) in affecting aqueous aggregation has become a topic of immense interest. Depending on the pH and the ionic strength of the solution many common porphyrins form J-aggregates in the presence of appropriate external additives. Effect of addition of a 'hydrophilic' IL, 1-butyl-3-methylimidazolium tetrafluoroborate ([bmim][BF_4]) on aqueous aggregation of a common porphyrin, tetrakis(4-sulfonatophenyl)porphyrin (TSPP), is investigated at different pH in the presence of varying concentration of [bmim][BF_4] using molecular absorbance and steady-state fluorescence. The kinetics of the interconverting species in the presence of [bmim][BF_4] within aqueous TSPP at different pH is also studied. It is observed that the low amount of [bmim][BF_4] (*ca.* 0.221–0.442 M or *ca.* 4.5–9.0 vol.%) favors the formation of J-aggregates at low solution pH; further increasing [bmim][BF_4] concentration leads to the destabilization of J-aggregates due to the deprotonation of TSPP from H_4TSPP^{2-} to H_2TSPP^{4-}, which, in turn, gets involved in formation of TSPP–[bmim][BF_4] complex. J-aggregation at low pH in the presence of [bmim][BF_4] is demonstrated to be significantly more efficient as compared to that in the presence of $NaBF_4$. Presence of [bmim][BF_4] at low pH facilitates the conversion of monomeric species to the J-aggregates which follows pseudo first-order kinetics with rate constants in agreement with experimental observations. Unique and effective role of IL [bmim][BF_4] in modifying aggregation behavior of aqueous TSPP is clearly demonstrated.

1. Introduction

Due to their unusual properties, ionic liquids (ILs) are garnering increased attention from academic and industrial research communities alike [1]. Almost every named synthesis and many more organic/inorganic/organometallic reactions have been reported in ILs [2,3]. Novel analytical applications of ILs are emerging every day; effective, and in some cases unique, utilizations of ILs have been demonstrated in a variety of techniques encompassing electroanalysis, separation, extraction, spectrometry, and sensing, among others [1,4–10]. Combined with the fact that ILs are composed entirely of cations and anions but still exist in the liquid state at ambient conditions, the recent investigations on ILs are partly also due to their *potential* environmentally benign nature. Most ILs have almost negligible vapor pressure and can be recycled easily. As a consequence, it is logical to employ these ILs in concert with other environmentally friendly systems such as supercritical fluids [11–14], aqueous [15–19] and surfactant-based systems [20–22].

Self-association of molecules plays a significant role in nature, particularly in living systems. Molecular aggregates of chlorophyll have been found to mediate the primary light harvesting and charge-transfer processes in photosynthetic complexes [23,24]. Among many molecular systems, the aggregate structure of cyanine and porphyrin dyes have garnered most attention due to the unique physiochemical properties associated with their aggregates [25,26]. Molecular aggregates of such dyes have been employed as potential organic photoconducters [27], as markers for biological and artificial membrane systems [28], as materials with enhanced non-linear optical properties [29,30] for use in non-linear optic devices [31,32] among others. Close-stacked molecular structure of aggregates may possess properties suitable for superconductivity, optical frequency conversion, and information processing and storage [33–35].

Porphyrins, a class of tetrapyrrolic dyes, have played an important role in medicinal chemistry over the last few decades due to their efficacy in photodynamic therapy (PDT) [36]. Some porphyrins and their complexes with paramagnetic metals have been used as potential fluorescence and magnetic resonance imaging (MRI) contrast agents as well [37]. The aggregation and dimerization of porphyrins and metalloporphyrins in aqueous solution have been widely investigated [38,39]. The phenomenon of aggregation of porphyrins in aqueous solution is highly dependent on the environmental characteristics, such as, ionic strength and pH; an appropriate combination of which may stimulate the aggrega-

* Corresponding author. Tel.: +91 11 26596503; fax: +91 11 26581102.
E-mail address: sipandey@chemistry.iitd.ac.in (S. Pandey).

1010-6030/$ – see front matter © 2009 Elsevier B.V. All rights reserved.
doi:10.1016/j.jphotochem.2009.07.022

tion process [40]. Among the aggregation studies of porphyrins, one may come across several reports focused on tetrakis-(4-sulfonatophenyl)-porphyrin (TSPP), where J-aggregates of the diacid form are observed in aqueous solution at low pH and high ionic strength [41]. It has been found that the counterion of inorganic salts, surfactant assemblies, microemulsions, metal ions, proteins, polypeptides, dendrimers, nucleic acids, cyclodextrins and myoglobin could promote the TSPP aggregation in acidic medium [42–48].

In recent investigations our group observed remarkable effectiveness of ILs in altering the physicochemical properties of aqueous surfactant systems, polymeric solutions, ethanol, water, and aqueous buffer solutions [49–59]. Interestingly, as demonstrated by us ILs show dual character in modifying properties of aggregates in aqueous solutions [49–55]. Specifically, at lower concentrations in aqueous media, ILs act similar to electrolytes though their effect on aggregation was observed to be significantly more dramatic as compared to that of common electrolytes. At higher concentrations, the cosolvent nature of ILs prevails. Consequently, it is imperative to investigate aggregation behavior of TSPP as IL is added in wide concentration range to the aqueous solution of TSPP. Further need to investigate aqueous TSPP aggregation in the presence of IL is warranted by ILs well-documented potential in changing the behavior of dye aggregation in aqueous solutions [60,61]. In this paper, we report the outcomes of our investigation on the effect of addition of a 'hydrophilic' IL 1-butyl-3-methylimidazolium tetrafluoroborate ([bmim][BF_4]) on aqueous TSPP aggregation at ambient conditions. In order to explore the aggregation behavior of TSPP, especially the J-aggregation, we have varied the pH of the solution as well as the concentration of [bmim][BF_4]. The efficiency and the kinetics of TSPP aggregation is studied using UV–vis molecular absorbance and steady-state fluorescence. Overall, our results demonstrate unique and effective role of IL [bmim][BF_4] in altering aqueous aggregation of this common porphyrin.

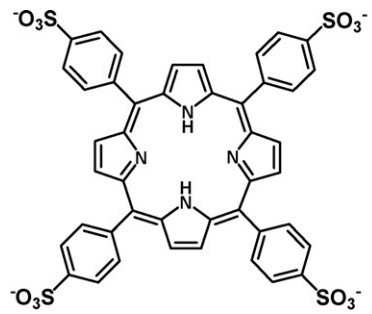

Tetrakis-(4-sulphonatophenyl)porphyrin (TSPP)

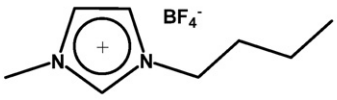

1-Butyl-3-methylimidazolium tetrafluoroborate ([bmim][BF_4])

Scheme 1. Tetrakis-(4-sulphonatophenyl)porphyrin (TSPP) 1-Butyl-3-methylimidazolium tetrafluoroborate ([bmim][BF_4]).

2. Experimental

2.1. Materials

Sodium salt of tetrakis(4-sulphonatophenyl)porphyrin (TSPP, high purity) was obtained from Sigma–Aldrich and was used as received. IL 1-butyl-3-methylimidazolium tetrafluoroborate ([bmim][BF_4], Merck, ultra pure, halide content <10 ppm, water content <10 ppm) was stored in dry conditions and was also used as received. Doubly distilled deionized water was obtained from a Millipore, Milli-Q Academic water purification system having $\geq$18 MΩ cm resistivity. Sodium tetrafluoroborate ($NaBF_4$) and hydrochloric acid (HCl) were obtained from Spectrochem Pvt. Ltd. and Qualigens, respectively. Ethanol (99.9%) was obtained from SD Fine-Chem. Ltd. Sodium dihydrogen orthophosphate and disodium hydrogen orthophosphate were purchased from Qualigens.

2.2. Methods

Stock solutions of TSPP were prepared in ethanol and water, respectively, and stored under refrigeration at 4 ± 1 °C in precleaned amber glass vials. Required amount of appropriate stock solution was taken and diluted to desired final concentration. Precalculated amount of [bmim][BF_4] was directly added to aqueous TSPP solution. pH adjustment was done with the help of aqueous HCl. In case of buffered TSPP samples, the solution was prepared in appropriate buffer solution. Phosphate buffer (50 mM) of pH 3.0 and 6.4 were prepared by proper combination of phosphoric acid, sodium dihydrogen orthophosphate and disodium hydrogen orthophosphate. Required amounts of materials were weighed using Mettler-Toledo AB104-S balance with a precision of $\pm$0.1 mg. A Perkin-Elmer Lambdabio 20 and a Systronics 2201 double beam spectrophotometer with variable bandwidth were used for the acquisition of UV–vis molecular absorbance data. Fluorescence spectra were acquired on model FL 3-11, Fluorolog-3 modular spectrofluorimeter with single Czerny-Turner grating excitation and emission monochromators having 450 W Xe arc lamp as the excitation source and a PMT as the detector purchased from Horiba-Jobin Yvon, Inc. All the data were acquired using 0.5- and 1-cm^2 path length quartz cuvettes. Spectral response from appropriate blanks was subtracted before data analysis. All data analysis was performed using Microsoft Excel and/or SigmaPlot 8.0 softwares.

3. Results and discussion

In aqueous solution, two or more chemical forms of TSPP may exist in equilibrium depending upon the pH of the solution. At lower pH, due to the protonation of the two pyrrole nitrogens of the ionic porphyrin (see Scheme 1) the biprotonated form (H_4TSPP^{2-}) predominates, whereas pH increase results in conversion of the biprotonated form into the monomeric base form (H_2TSPP^{4-}). The pK_a of this aqueous prototropic equilibrium is reported to be ~4.8 at 25 °C and ambient conditions [62].

3.1. Electronic absorbance of aqueous TSPP in the presence of [bmim][BF_4]

The electronic absorption spectrum of the deprotonated species, H_2TSPP^{4-}, shows an intense Soret band (B band) in the high energy region at 414 nm and four weak Q bands at 515, 551, 580 and 645 nm for 0–0 and 0–1 vibronic components. Molecular symmetry of this form of the compound is D_{2h}. However, due to the protonation at low pH (i.e., at pH < 4.8) the symmetry of the compound increases to D_{4h} and is manifested via a dramatically changed absorption pattern which shows the Soret band shifted bathochromically to 434 nm and the three Q bands located at 550, 593 and 645 nm corresponding to the biprotonated species, H_4TSPP^{2-} [40,62]. Most importantly, depending on pH, ionic strength and concentration of porphyrin, among others, TSPP shows interesting aggregation behavior by forming J- and/or H-aggregates in which the monomer transition dipoles are aligned

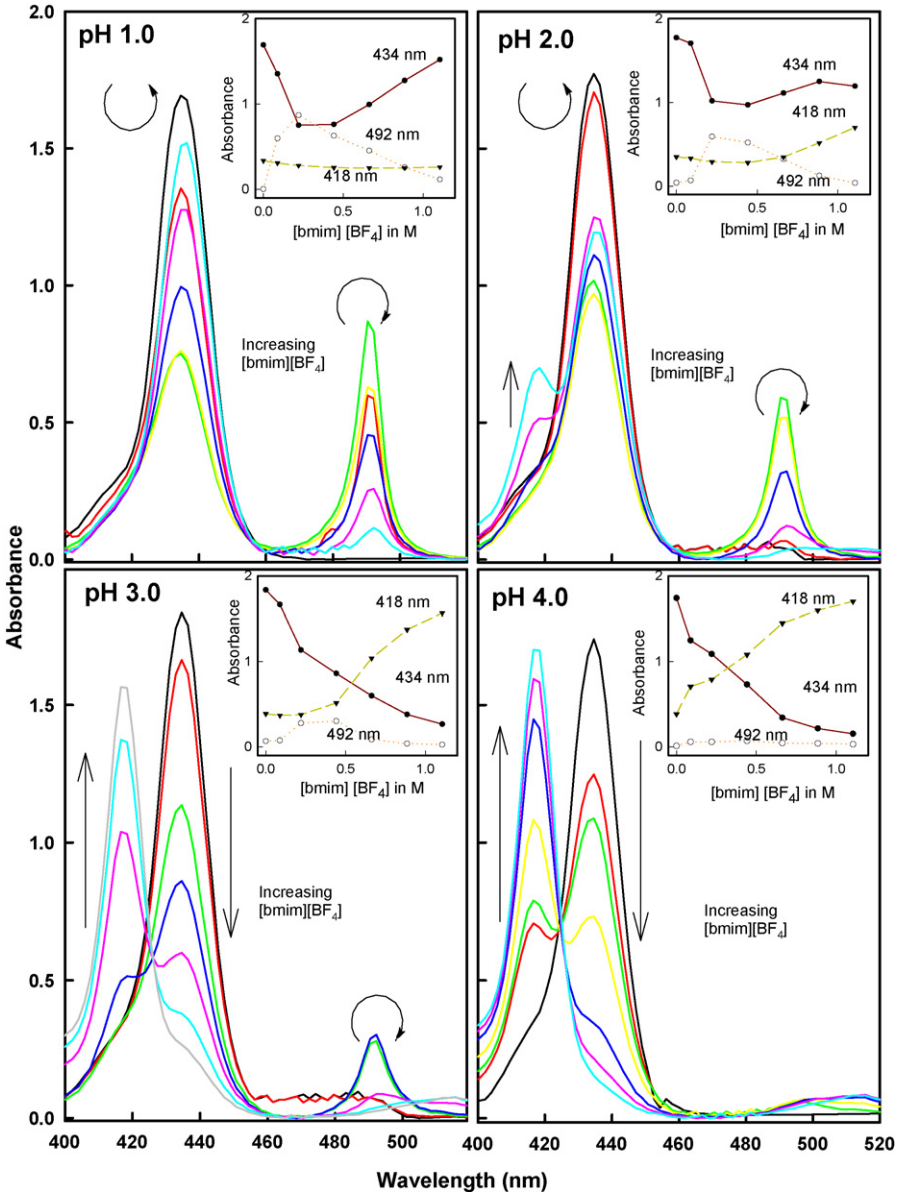

Fig. 1. Absorbance spectra of TSPP (50 μM) in aqueous HCl in the presence of different concentrations of [bmim][BF_4] (0–1.1 M) at ambient conditions. pH 1.0, 2.0, 3.0, and 4.0, respectively, are the initial solution pH in the absence of [bmim][BF_4]. Insets show absorbance of TSPP *versus* [bmim][BF_4] concentration at 418 nm (- - - -), 434 nm (—), and 492 nm (· · · · ·).

parallel and perpendicular to the hypothetical line connecting adjacent porphyrin molecules in the aggregates, respectively [25].

We investigated electronic absorbance behavior of aqueous TSPP in the presence of varying concentration of hydrophilic IL [bmim][BF_4] at several pH ranging from highly acidic (i.e., pH 1.0) to neutral. Fig. 1 presents absorbance spectra of TSPP in the presence of different concentrations of [bmim][BF_4] when pH of the solution in the absence of [bmim][BF_4] is below the threshold pH of 4.8; specifically, pH 1.0, 2.0, 3.0, and 4.0. It is important to mention that the requisite pH of the above solutions are achieved using HCl. While the energy of all absorbance transitions of TSPP in this pH region in our investigation are in agreement with that reported in literature [63], we are only focusing on high energy Soret bands to assess the effect of addition of IL [bmim][BF_4] on TSPP aggregation. A careful examination of Fig. 1 reveals several noteworthy outcomes regarding the effect of IL [bmim][BF_4] on aqueous TSPP aggregation. As documented in the literature, the high energy spectral region is mainly characterized by three absorbance bands around 434, 491, and 418 nm representing H_4TSPP^{2-} monomers, J-aggregates, and TSPP–[bmim][BF_4] complex (formed due to the electrostatic attractive interaction between anionic sulfonates of TSPP and $bmim^+$ of the IL), respectively [45]. It is interesting to note that as [bmim][BF_4] is added to pH 1.0 solution of TSPP, the absorbance at 434 nm decreases to a minima before increasing while that at 491 nm increases to a maxima before decreasing clearly indicating the increased efficiency of J-aggregation in the presence of up to 0.221–0.442 M [bmim][BF_4] (or 4.5–9.0 vol.%). Further increase of [bmim][BF_4] concentration up to 1.769 M (or 35.7 vol.%) appears to result in conversion of the J-aggregates back to the monomeric form of TSPP (inset, top left panel, Fig. 1). High concentration of [bmim][BF_4] appears to destabilize the J-aggregates. At pH 2.0, the trends in absorbance at 434 nm and that at 491 nm are similar to those at pH 1.0, except for an increase in the absorbance at 418 nm for [bmim][BF_4] > 0.442 M (or 9.0 vol.%) indicating a more facile formation of TSPP–[bmim][BF_4] complex at higher concentrations of [bmim][BF_4]. It is suggested that a frac-

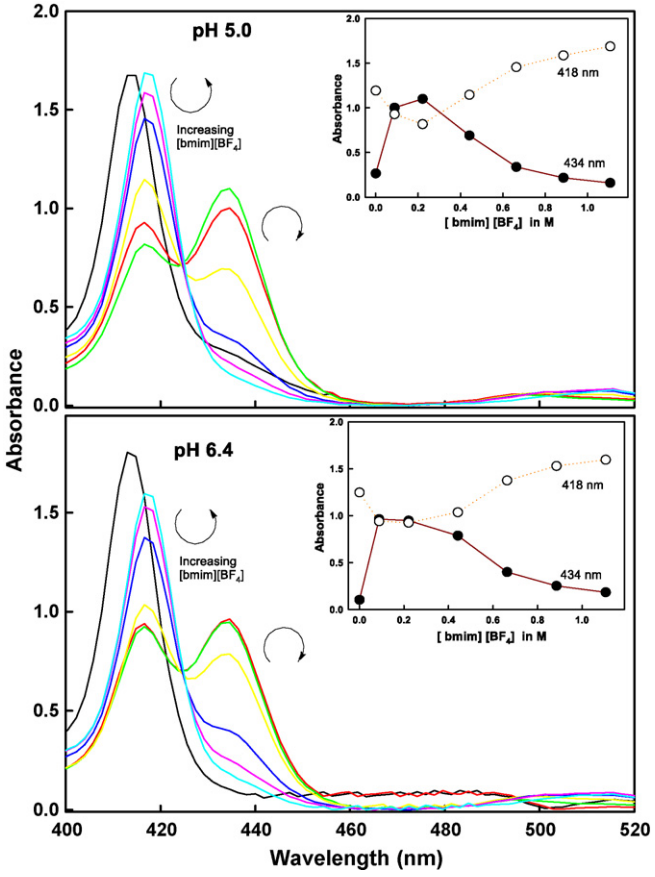

Fig. 2. Absorbance spectra of TSPP (50 μM) in aqueous HCl (top panel) and in neat water (bottom panel) in the presence of different concentrations of [bmim][BF_4] (0–1.1 M) at ambient conditions. pH 5.0 and 6.5, respectively, are the initial solution pH in the absence of [bmim][BF_4]. Insets show absorbance of TSPP *versus* [bmim][BF_4] concentration at 418 nm (·····) and 434 nm (—).

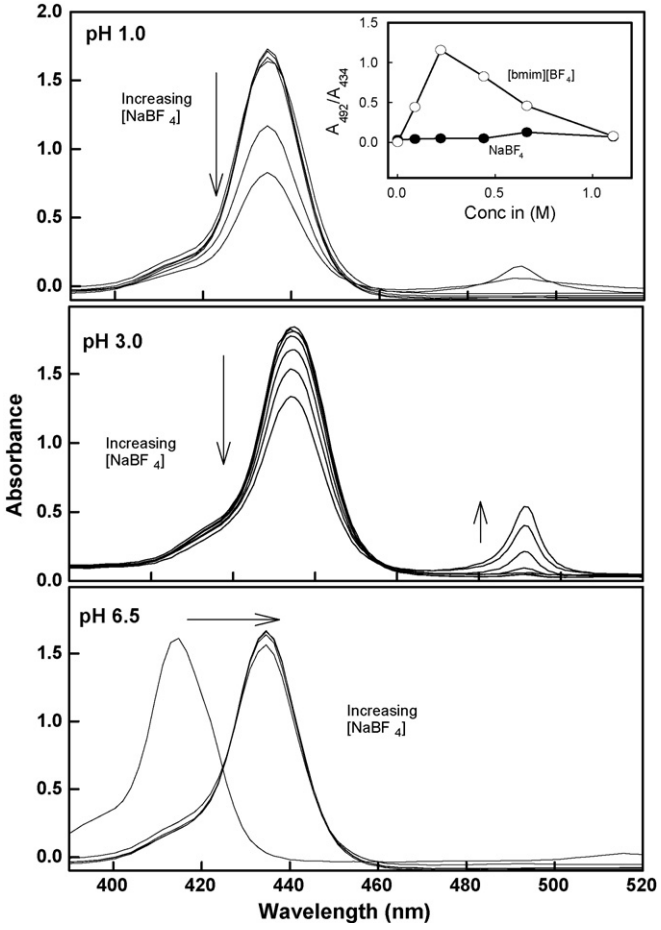

Fig. 3. Absorbance spectra of TSPP (50 μM) in aqueous HCl (top and middle panels) and in neat water (bottom panel) in the presence of different concentrations of $NaBF_4$ (0–1.1 M) at ambient conditions. pH 1.0, 3.0, and 6.5, respectively, are the initial solution pH in the absence of $NaBF_4$. Inset shows efficiency of J-aggregation in terms of the ratio of TSPP absorbance values at 492–434 nm *versus* the additive concentration for [bmim][BF_4] (○) and $NaBF_4$ (●), respectively.

tion of TSPP may deprotonate at higher [bmim][BF_4] concentrations thus forming TSPP–[bmim][BF_4] complex in the solution. Deprotonation of TSPP upon its interaction with cationic micelles even at low pH is proposed in literature earlier [64], even the presence of cyanine with hexyl chains [65] and certain drug-carrier proteins [66] also show this effect. The increase after the minima in 434 nm absorbance is not as dramatic at pH 2.0 as that observed at pH 1.0 (inset, top right panel, Fig. 1). TSPP–[bmim][BF_4] complex appears to be not so favorable at pH 1.0 perhaps due to the absence of significant amount of deprotonated TSPP even at high [bmim][BF_4] concentrations as the pH is too low. To our convenience, the absorbance at 418 nm shows significant increase indicating increased formation of TSPP–[bmim][BF_4] complex upon [bmim][BF_4] addition to pH 3.0 and pH 4.0 solutions of TSPP, respectively (lower panels, Fig. 1). Subsequently, the absorbance at 434 nm shows a monotonic decrease at these two pH. While the maxima in 492 nm absorbance showing the J-aggregates is still observed at pH 3.0 (the maximum absorbance is significantly lower as compared to that at pH 1.0 and 2.0), this band almost vanishes at pH 4.0 indicating negligible presence of J-aggregates at pH 4.0 irrespective of [bmim][BF_4] concentration.

Absorbance spectra of TSPP above the threshold pH, at pH 5.0 (aqueous HCl) and pH 6.5 (neat water) in the absence of [bmim][BF_4] and after [bmim][BF_4] addition are presented in Fig. 2. In the absence of [bmim][BF_4], the absorbance of the basic form H_2TPPS^{4-} is characterized by the Soret peak at ~414 nm in accordance with the literature [40,62]. Addition of [bmim][BF_4], however, results in bathochromic shift of this peak to ~418 nm accompanied by a reduction in absorbance to a minima at ~0.221 M (or ~4.5 vol.%) [bmim][BF_4] before increasing again upon further addition of IL to 1.106 M (or 22.32 vol.%). Surprisingly, the absorbance at ~434 nm increases to a maxima upon addition of up to ~0.221 M (or ~4.5 vol.%) [bmim][BF_4] before decreasing on further addition of IL. It appears that, at higher pH, J-aggregates do not form and the presence of [bmim][BF_4] facilitates formation of TSPP–[bmim][BF_4] complex; the rise and subsequent decline of the absorbance band characteristics of H_4TSPP^{2-} monomers upon IL addition is not easy to conceive at first. However, we realized the well-documented hydrolytic instability of ILs [19], and consequently measured the pH of neat water and aqueous HCl solution having pH 5.0, respectively, as [bmim][BF_4] is added (Figure S1). It is clear that addition of [bmim][BF_4] decreases the pH of the solution; pH of 0.088 M aqueous [bmim][BF_4] solution is 4.1 (±0.1), which is below the threshold pH of 4.8. It is obvious that protonated form of TSPP monomers, i.e., H_4TSPP^{2-}, are produced as [bmim][BF_4] is added. It is important to mention that for 0.221 M (or 4.5 vol.%) ≤ [bmim][BF_4] ≤ 1.106 M (or 9.0 vol.%), the decrease in the pH of the solution is not as significant (Figure S1), which may explain the decrease in the absorbance at 434 nm in this range as more deprotonated TSPP would form as the concentration of [bmim][BF_4] is increased (this, in turn, forms TSPP–[bmim][BF_4] complex characterized by the band at 418 nm). This is further verified by collecting absorbance spectra when [bmim][BF_4] is added to

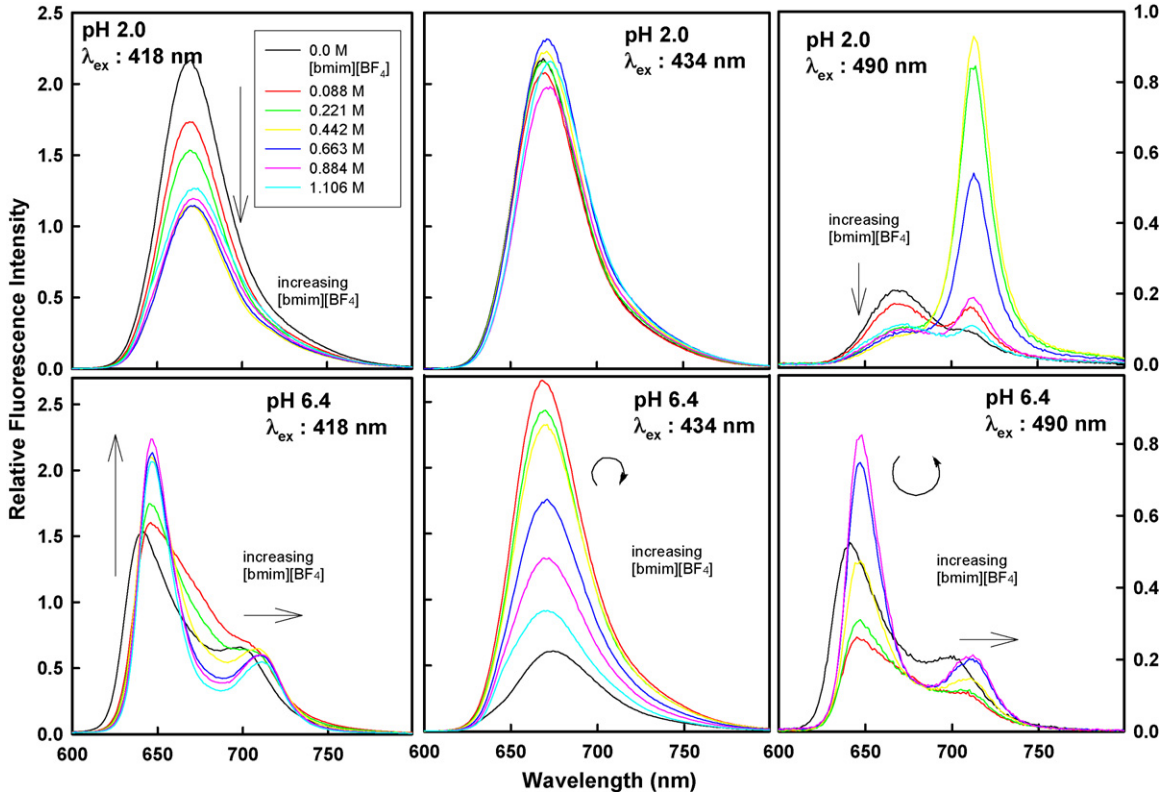

Fig. 4. Fluorescence emission spectra of TSPP (5 μM) in aqueous HCl (top three panels) and in neat water (bottom three panels) in the presence of different concentrations of [bmim][BF_4] (0–1.1 M) at ambient conditions. pH 2.0 and 6.4, respectively, are the initial solution pH in the absence of [bmim][BF_4].

pH 3.0 acetate buffer and pH 6.5 phosphate buffer solution of TSPP, respectively (Figure S2). While the absorbance behavior of buffered pH 3.0 TSPP solution is very similar to that of aqueous HCl pH 3.0 TSPP solution, no presence of absorbance at ~434 nm clearly suggests the absence of protonated monomeric H_4TSPP^{2-} irrespective of the amount of [bmim][BF_4] added (please also refer to Figure S1).

It is important to compare the effect of IL [bmim][BF_4] on aqueous aggregation of TSPP with that of $NaBF_4$ to highlight the specific role of IL, if any, on such aggregation. Fig. 3 presents absorbance spectra of aqueous TSPP solutions at pH 1.0 (attained using HCl, top panel), pH 3.0 (attained using HCl, middle panel), and pH 6.5 (neat water, lower panel) and as $NaBF_4$ is added to these solutions. A clear difference in the efficiency of J-aggregate formation is seen; in comparison to [bmim][BF_4], addition of $NaBF_4$ results in insignificant formation of J-aggregates. Similarly, at pH 3.0, unlike the result of addition of [bmim][BF_4], no formation of TSPP–[bmim][BF_4] complex is seen. Interesting difference in TSPP absorbance behavior is also observed in neat water. Addition of both [bmim][BF_4] and $NaBF_4$, respectively, results in considerable lowering of the pH of the solution (Figure S1) that should favor H_4TSPP^{2-} at the expense of H_2TSPP^{4-}. However, while addition of [bmim][BF_4] to TSPP in neat water promotes TSPP–[bmim][BF_4] complexation (Fig. 2) along with increase and subsequent decrease in H_4TSPP^{2-} concentration (i.e., absorbance at ~434 nm), addition of $NaBF_4$ results in almost quantitative conversion of H_2TSPP^{4-} to H_4TSPP^{2-}; no discernible presence of any complex could be observed (lower panel, Fig. 3). Unique effect of IL [bmim][BF_4] on aqueous aggregation of TSPP is clearly established.

It is important to mention that Liu and co-workers have also reported facilitation of J-aggregates of diprotonated TSPP as IL [bmim][BF_4] is added; however, their investigation is restricted to solutions of only pH 2.24 and 5.82 [67]. Further, the maximum concentration of IL [bmim][BF_4] was only 0.40 M or 8 vol.% in their studies at which the ILs usually act similar to electrolytes and their behavior is devoid of any cosolvent-like characteristics. Most importantly, well-documented hydrolytic instability of IL [bmim][BF_4] did not feature in any of their data interpretation.

Further, we have investigated the effect of TSPP concentration on its aggregation in the presence of IL [bmim][BF_4]. For this, [TSPP] is increased up to 100 μM at pH 1.0 (Figure S3), pH 3.0 (Figure S4), and pH 6.5 (Figure S5), respectively, in the presence of up to 1.106 M (or 22.3 vol.%) IL [bmim][BF_4]. Many interesting features are noteworthy. At pH 1.0, increasing [TSPP] in the absence of [bmim][BF_4] with negligible J-aggregation still does not result in any J aggregate formation. In the presence of 0.088 M (1.8 vol.%) and 0.221 M (4.5 vol.%) [bmim][BF_4], where J-aggregation is most efficient, increasing [TSPP] results in J-aggregate formation with increased efficiency (A_{494}/A_{434} increases with increasing [TSPP]). An increase in [TSPP] results in growing shoulder at 418 nm clearly implying formation of TSPP–[bmim][BF_4] complex irrespective of [bmim][BF_4] concentration. All three bands centered at 418, 434, and 492 nm show increased absorbance as [TSPP] is increased at pH 3.0. Similar observations are recorded at pH 6.5 where absorbance values at 414 or 418 nm as well as those at 434 nm increase with increasing [TSPP], however, in the presence of 0.088 M (1.8 vol.%) and 0.221 M (4.5 vol.%) [bmim][BF_4], formation of J-aggregates is also clearly visible (i.e., the appearance of band at 492 nm) at higher [TSPP].

3.2. *Molecular fluorescence of aqueous TSPP in the presence of [bmim][BF_4]*

Fluorescence emission spectra of aqueous TSPP in the absence and presence of [bmim][BF_4] were obtained at pH 2.0 and pH 6.4, respectively. Fig. 4 presents variation in fluorescence emission behavior of 5 μM aqueous TSPP as [bmim][BF_4] is added

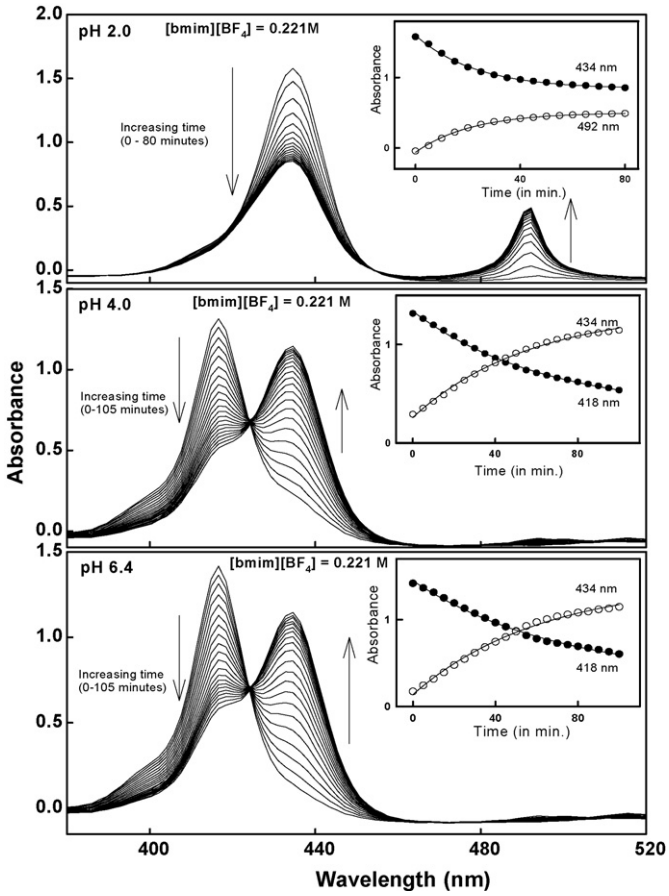

Fig. 5. Time-dependent absorbance spectra of TSPP (50 μM) in aqueous HCl (top and middle panels) and in neat water (bottom panel) in the presence of 0.221 M [bmim][BF_4] at ambient conditions. pH 2.0, 4.0, and 6.4, respectively, are the initial solution pH in the absence of [bmim][BF_4]. Insets show change in absorbance of TSPP at 418, 434, and 492 nm, respectively, with time.

when excited at 418, 434, and 490 nm, respectively. At pH 2.0 (the top three panels in Fig. 4) a broad emission peak appears at ~670 nm irrespective of the excitation wavelength. This is assigned to the 0–0 transition of the diprotonated TSPP and the fluorescence intensity follows the same trend as absorbance values at pH 2.0 (Fig. 1); no distinct change in emission peak for TSPP–[bmim][BF_4] complex appears perhaps due to the low concentration of TSPP–[bmim][BF_4] complex as compared to the concentration of diprotonated species. No clear trend in fluorescence intensity is observed for $\lambda_{excitation}$ = 434 nm. This is in concert with the changes in the absorbance values with the addition of [bmim][BF_4] at this wavelength (*vide supra*). The fluorescence emission behavior is considerably different when the aqueous TSPP solution in the absence and presence of [bmim][BF_4] are excited at 490 nm (i.e., corresponding to the J-aggregates). Clearly, the emission spectra are characterized by the presence of an additional sharp band at ~710 nm. The origin of this band is attributed to the J-aggregates; the emission intensity of this new band follows the same trend as that observed for the absorbance values at 490 nm. Presence of J-aggregates and the effect of [bmim][BF_4] addition on J-aggregates are confirmed independently by molecular fluorescence.

Fluorescence behavior of [bmim][BF_4]-added aqueous TSPP at pH 6.4 (neat water) is significantly different. It is important to keep in mind the decrease in solution pH upon addition of IL [bmim][BF_4]; IL renders the solution acidic (Figure S1). As expected, fluorescence emission spectra for $\lambda_{excitation}$ = 434 nm is similar to that observed at pH 2.0 with trend in fluorescence intensity of the band representing monomeric TSPP (at ~670 nm) is similar to that of the absorbance values (refer to Fig. 2). The fluorescence behavior at $\lambda_{excitation}$ = 418 nm and that at $\lambda_{excitation}$ = 490 nm are different; fluorescence emission spectra show two bands. The higher energy band shows a maxima ~640 nm in the absence of [bmim][BF_4] which shifts bathochromically ~10 nm in the presence of [bmim][BF_4] at both excitation wavelengths. This band is assigned to the 0–0 transition in the literature [66] and the bathochromic shift in the presence of [bmim][BF_4] may be attributed to the presence of TSPP–[bmim][BF_4] complex (similarities are stark with UV–vis molecular absorbance behavior, *vide supra*). The lower energy band, however, is assigned to the 0–1 vibronic transition [66], and as the concentration of [bmim][BF_4] is increased in the solution, this band also demonstrates a gradual bathochromic shift. This shift may also be assigned to the presence of TSPP–[bmim][BF_4] complex. Similar observations were reported earlier for TSPP as its concentration was increased in the solution [68]. A careful examination of our overall fluorescence data reveals that this emission feature corresponding to 0–1 vibronic transition shows up in the all fluorescence spectra of aqueous TSPP irrespective of pH and the concentration of [bmim][BF_4]; it appears as a shoulder at ~710 nm imparting asymmetry to the fluorescence band. It also appears that the fluorescence band due to 0–1 vibronic transition overlaps with the one due to the J-aggregation. The fact that the formation of J-aggregates at pH 6.4 due to the addition of [bmim][BF_4] (the J-aggregates due to lowered pH, which UV–vis molecular absorbance is not sensitive enough to show) is responsible for the band at ~710 nm may not be completely ruled out. However, the appearance of this band when excited at 418 nm renders this proposition lesser weight. All-in-all, fluorescence behavior of aqueous TSPP in the presence of [bmim][BF_4] appears to complement the UV–vis absorbance behavior, but also affords additional information at much lower TSPP concentration due to the inherently high sensitivity associated with the fluorescence technique.

3.3. *Effect of [bmim][BF_4] addition on time-dependent aggregation of aqueous TSPP*

One of the important features of TSPP aggregation is its time-dependent behavior. It is well-established that the aggregation kinetics depends on inter-particle interactions, which are controlled by the ionic strength or the pH [40]. Our aim is to investigate the kinetics of the aggregation of aqueous TSPP at different pH in the presence of IL [bmim][BF_4]. Toward this end, kinetic study of the aggregation of TSPP was carried out in the presence of 0.221 M (4.5 vol.%) and 0.884 M (17.8 vol.%) [bmim][BF_4] at three different pH, 2.0, 4.0, and 6.4, by measuring the UV–vis molecular absorbance of TSPP. Time-dependent UV–vis molecular absorbance spectra of TSPP (50 μM) in the presence of 0.221 M (or 4.5 vol.%) [bmim][BF_4] at three different pH are presented in Fig. 5. A cursory examination of the data presented in Fig. 5 amply demonstrates the inter-conversion of the different forms of TSPP within the temporal domain of the investigation. It is important to mention that no such behavior is observed in the absence of [bmim][BF_4]; i.e., absorbance behavior of aqueous TSPP at pH 2.0 and at pH 6.4 remains almost unaltered within the same temporal domain (Figure S6). It is confirmed, therefore, that the time-dependent evolution and decay of species within [bmim][BF_4]-added aqueous TSPP solutions is due to the presence of IL [bmim][BF_4].

At pH 2.0 the monomeric diprotonated H_4TSPP^{2-} changes to the J-aggregates with time and a clear isobestic point is observed at ~455 nm. The inset of Fig. 5 (top panel) shows the build up of J-aggregates (monitored by the absorbance at 492 nm) and decay of monomeric diprotonated H_4TSPP^{2-} (monitored by the absorbance at 434 nm). In the presence of 0.221 M (or 4.5 vol.%) [bmim][BF_4], the decay of the monomeric species as well as

Table 1
Recovered rate constants from fitting the data presented in Fig. 5 to Eq. (1) or (2). Goodness-of-the-fit in terms of r^2 is also provided.

	Equation	k (min^{-1})	r^2
pH 2.0			
Absorbance at 492 nm	(1)	$4.67(\pm0.18)\times10^{-2}$	0.9971
Absorbance at 434 nm	(2)	$4.36(\pm0.16)\times10^{-2}$	0.9976
pH 4.0			
Absorbance at 434 nm	(1)	$1.76(\pm0.11)\times10^{-2}$	0.9968
Absorbance at 418 nm	(2)	$1.57(\pm0.08)\times10^{-2}$	0.9983
pH 6.4			
Absorbance at 434 nm	(1)	$1.62(\pm0.12)\times10^{-2}$	0.9960
Absorbance at 418 nm	(2)	$1.42(\pm0.11)\times10^{-2}$	0.9964

the growth of J-aggregates may be considered pseudo-first order ($0.221\,M \gg 5\times10^{-5}\,M$) in nature. Since the absorbance at 492 nm is almost entirely due to J-aggregates (*vide supra*), a simple kinetic scheme furnishes the following expression:

$$A^{492\,nm} = \varepsilon_J^{492\,nm}[J]_0 + \varepsilon_M^{492\,nm}[M]_0(1-e^{-kt}) \quad (1)$$

where J and M stand for the J-aggregates and the monomeric species, respectively, and the k is the pseudo first-order rate constant for the formation of J-aggregates from the monomeric species. A more generalized scheme, however, is used for the decrease in absorbance at 434 nm as it may not be solely due to the decay of monomeric species:

$$A^{434\,nm} = \varepsilon_M^{434\,nm}[M]_0e^{-kt} + \varepsilon_J^{434\,nm}[M]_0(1-e^{-kt}) + \varepsilon_J^{434\,nm}[J]_0 \quad (2)$$

Subsequently, the variation in absorbance at 492 nm and that at 434 nm with time were fitted to $y = y_{0,1} + a_1(1-e^{-kt})$ and $y = y_{0,2} + a_2\,e^{-kt}$, respectively. The dark curves in the inset of Fig. 5 (top panel) show the results of the fit, which appear to be satisfactory. Table 1 presents recovered rate constants k, the parameter of utmost importance to us, along with the goodness-of-the-fit in terms of r^2. The most noteworthy point here is the excellent agreement between the rate constant k recovered from the decay of the monomeric species to that from the growth of the J-aggregates [$4.36(\pm0.16)\times10^{-2}$ min^{-1} *versus* $4.67(\pm0.18)\times10^{-2}$ min^{-1}]. Costa et al. have reported similar rate constants for HSA-catalyzed monomer to J-aggregate conversion for TSPP [46]. In another report, Pasternack and coworkers have reported the rate constants from the measurements at 491 nm and 435 nm for 3.61 μM TSPP at pH 0.5 to be 4.5×10^{-2} min^{-1} and 5.34×10^{-2} min^{-1}, respectively [69].

Increasing the concentration of [bmim][BF_4] to 0.884 M (17.8 vol.%) reduces the efficiency of J-aggregate formation within aqueous TSPP solution at pH 2.0 (*vide supra*). Insignificant growth of the absorbance band at 492 nm in our temporal domain renders the efforts to investigate the kinetics of TSPP aggregation within 0.884 M (17.8 vol.%) [bmim][BF_4]-added solution at pH 2.0 futile (Figure S7). In fact, a decrease in the absorbance band at 418 nm (corresponding to TSPP–[bmim][BF_4] complex) gives rise to an increase in the band at 434 nm (corresponding to the monomeric species) at this [bmim][BF_4] concentration within the temporal domain of the investigation.

In the presence of 0.221 M (or 4.5 vol.%) [bmim][BF_4] within the aqueous TSPP solutions at pH 4.0 and pH 6.4, respectively, the species corresponding to the absorbance band at 418 nm (i.e., the TSPP–[bmim][BF_4] complex) gradually changes to monomeric species (absorbance band at 434 nm) and clear isobestic points are observed at 424 nm (Fig. 5). Arguing similarly as above, the growth and decay in the absorbance values at 434 and at 418 nm, respectively, are fitted to equations similar to Eqs. (1) and (2) above. The results of the fits are presented within the insets of the middle and the lower panels of Fig. 5 by dark curves and the relevant recovered parameters are reported in Table 1. The fits are satisfactory; more importantly, the recovered rate constants are in excellent agreement with each other [$1.57(\pm0.08)\times10^{-2}$ min^{-1} *versus* $1.76(\pm0.11)\times10^{-2}$ min^{-1} at pH 4.0 and $1.42(\pm0.11)\times10^{-2}$ min^{-1} *versus* $1.62(\pm0.12)\times10^{-2}$ min^{-1} at pH 6.4]. Again, in the absence of IL [bmim][BF_4] no such change is observed (Figure S6). Similar to what was observed at pH 2.0, in the presence of 0.884 M (or 17.8 vol.%) [bmim][BF_4] the changes in the absorbance values are insignificant (Figure S7). The reason for the similarity of the kinetic data for TSPP aggregation at pH 4.0 and 6.4 is the lowering of the solution pH in the presence of IL [bmim][BF_4] (Figure S1). In fact, the pH of the solutions initially having pH of 6.4 (neat water) and 4.0 (using HCl) were measured in the presence of 0.221 M (or 4.5 vol.%) [bmim][BF_4] and were found to be ~3.5 and ~3.4, respectively. This nicely explains the similarities in the recovered rate constants at two pH values (Table 1).

3.4. Role of [bmim][BF_4] in affecting aqueous aggregation of TSPP

It is well documented that the most important requirement for aqueous TSPP aggregation is the presence of ions along with the protonation of the inner N atoms [63,70–73]. Specifically, J-aggregation is known to take place at low pH aqueous TSPP solutions of high ionic strength [41,46]. It is clear from our investigation that while only low pH or high concentration of ions alone is not sufficient to induce J-aggregation, high concentration of IL [bmim][BF_4] appears to result in efficient formation of TSPP–[bmim][BF_4] complex. Addition of IL [bmim][BF_4] increases the efficiency of both J-aggregation as well as TSPP–[bmim][BF_4] complex formation processes within aqueous TSPP. While the formation efficiency of TSPP–[bmim][BF_4] complex, in general, appears to become more and more favorable as the [bmim][BF_4] concentration is increased up to ~1.106 M (or ~22.3 vol.%) within the solutions above pH 1.0, J-aggregates surprisingly become less stable at higher [bmim][BF_4] concentrations. It is clear from our investigation that J-aggregates evolve from the diprotonated TSPP, i.e., H_4TSPP^{2-}, in the solution even at moderate to high initial pH as addition of [bmim][BF_4] results in lowering of the solution pH (Figure S1) thus facilitating the existence of H_4TSPP^{2-}. The presence of diprotonated species H_4TSPP^{2-} appears to be mandatory for the formation of J-aggregates. It is evident from our overall data that the TSPP–[bmim][BF_4] complex is formed predominantly as a result of direct interaction between the IL [bmim][BF_4] and H_2TSPP^{4-} in the solution. Whether the IL [bmim][BF_4] exists in dissociated or associated form within the solution also appears to be of not much importance as far as TSPP–[bmim][BF_4] complex formation is concerned.

J-aggregates, due to their inherent unique features and widespread applications, are relatively of more importance. Presence of diprotonated form of TSPP, H_4TSPP^{2-}, is deemed essential for the formation of J-aggregates [70–72]. Upon protonation, TSPP is converted from a configuration in which the aryl moiety is twisted relative to the macrocycle plane to one in which it is nearly coplanar. In the presence of appropriate inducing agents, these coplanar H_4TSPP^{2-} may rearrange in a fashion with a displacement between the next nearest neighbor such that oppositely charged sites are positioned closed to one another (head-to-tail alignment of the transition dipole moments). The strong coulombic attraction between the positively charged macrocycles and the negatively charged sulfonate groups of neighboring molecules contribute to stabilize these J-aggregates. Both of these requirements are in fact necessary, since a planar conformation undoubtedly creates a favorable condition for close contact of vicinal molecular species, while negative site can allow for strong energy-lowering interaction with positive sites [70]. However, it is well-documented that this would only take place in the presence of enough concentration of appropriate ionic species in the solution [70–75]. Therefore,

a balanced combination of both hydrophobic π–π stacking interaction as well as coulombic electrostatic attractive interaction is essential for the formation of J-aggregates. IL [bmim][BF_4] appear to fulfill these requirements in an effective fashion.

At low pH, the presence of [bmim][BF_4] introduces remarkable changes in the spectroscopic features of TSPP. At moderate concentrations, the bulky organic cation $bmim^+$ of IL [bmim][BF_4] (Scheme 1) may provide a positive micro-phase distinct from the aqueous bulk, which reduces the electrostatic repulsion between the two TSPP moieties and induce aggregation by helping in π–π stacking because of structural similarities. Further addition of [bmim][BF_4] causes deprotonation of TSPP converting H_4TSPP^{2-} (D_{4h}) to H_2TSPP^{4-} (D_{2h}) in which the aryl moieties are twisted out-of-plane thus destabilizing the J-aggregates formed. The balance between electrostatic and hydrophobic mutual interactions is now disturbed to an extent such that J-aggregates are no longer stabilized at higher [bmim][BF_4] concentrations and the TSPP–[bmim][BF_4] interaction prevails giving rise to TSPP–[bmim][BF_4] complex formation showing absorption peak at 418 nm. The formation of TSPP–[bmim][BF_4] complex from H_2TSPP^{4-} is further confirmed as very low concentration of [bmim][BF_4] (*ca.* 0.012 M or *ca.* 0.24 vol.%) is added to the solution of pH 6.4 where TSPP exists only in deprotonated form. The TSPP–[bmim][BF_4] complex formation appears to be pH-dependent as the absorbance at ~418 nm corresponding to this complex becomes more at higher pH (Fig. 1) with the same concentration of IL due to the higher concentration of the deprotonated form at higher pH.

Formation of J-aggregates by TSPP can be achieved in the presence of high concentrations of cations including K^+ and H^+ [41,71], and in the presence of surfactants [71], which were able to induce aggregation at a higher rate than cations below the critical micelle concentration (cmc). The presence of proteins such as Human Serum Albumin (HSA) and β-lactoglobulin [46] is also known to facilitate the J-aggregation process. Aggregation was also reported in confined media, e.g., aluminosilicate mesostructure, adsorbed polycation films and TiO_2 nanoparticles [73–75]. In the context of these results, IL [bmim][BF_4] has a unique role in affecting aqueous aggregation of TSPP; the addition of up to ~0.221 M [bmim][BF_4] first facilitates the J-aggregation process, however, further increase in IL concentration destabilizes the J-aggregates. Complexation between the bulky IL cation $bmim^+$ and sulfonates of TSPP also plays a crucial role as excess of [bmim][BF_4] appears to help deprotonate TSPP even within moderately low pH solutions.

Acknowledgements

This work was generously funded by a grant to SP from the Department of Science and Technology (DST), Government of India (grant no. SR/S1/PC-16/2008). MA would like to thank UGC, India for a fellowship.

Appendix A. Supplementary data

Supplementary data associated with this article can be found, in the online version, at doi:10.1016/j.jphotochem.2009.07.022.

References

[1] G.A. Baker, S. Baker, S. Pandey, F.V. Bright, Analyst 130 (2005) 800.
[2] P. Wasserscheid, T. Welton (Eds.), Ionic Liquids in Synthesis, Wiley–VCH, Weinheim, Germany, 2003.
[3] T. Welton, Chem. Rev. 99 (1999) 2071.
[4] S. Pandey, Anal. Chim. Acta 556 (2006) 38.
[5] R.D. Rogers, K.R. Seddon (Eds.), Ionic Liquids: Industrial Applications for Green Chemistry, ACS Symposium Series, vol. 818, American Chemical Society, Washington, DC, 2002.
[6] R.D. Rogers, K.R. Seddon (Eds.), Ionic Liquids as Green Solvents: Progress and Prospects, ACS Symposium Series, vol. 856, Washington, DC, American Chemical Society, 2003.
[7] R.D. Rogers, K.R. Seddon (Eds.), Ionic Liquids III: Fundamentals, Challenges, and Opportunities, ACS Symposium Series, American Chemical Society, Washington, DC, 2005.
[8] H. Ohno (Ed.), Electrochemical Aspects of Ionic Liquids, Wiley–Interscience, 2005.
[9] C.F. Poole, J. Chromatogr. A 1037 (2004) 49.
[10] H. Jin, B. O'Hare, J. Dong, S. Arzhantsev, G.A. Baker, J.F. Wishart, A.J. Benesi, M. Maroncelli, J. Phys. Chem. B 112 (2008) 81.
[11] L.A. Blanchard, J.F. Brennecke, Ind. Eng. Chem. Res. 40 (2001) 287.
[12] A.M. Scurto, S.N.V.K. Aki, J.F. Brennecke, J. Am. Chem. Soc. 124 (2002) 10276.
[13] L.A. Blanchard, D. Hancu, E.J. Beckman, J.F. Brennecke, Nature 399 (1999) 6731.
[14] S.N. Baker, G.A. Baker, M.A. Kane, F.V. Bright, J. Phys. Chem. B 105 (2001) 9663.
[15] K.A. Fletcher, S. Pandey, Appl. Spectrosc. 56 (2002) 266.
[16] S. Pandey, K.A. Fletcher, S.N. Baker, G.A. Baker, Analyst 129 (2004) 569.
[17] S.N. Baker, G.A. Baker, F.V. Bright, Green Chem. 4 (2002) 165.
[18] S.N. Baker, G.A. Baker, C.A. Munson, F. Chen, E.J. Bukowski, A.N. Cartwright, F.V. Bright, Ind. Eng. Chem. Res. 42 (2003) 6457.
[19] G.A. Baker, S.N. Baker, Aust. J. Chem. 58 (2005) 174.
[20] K.A. Fletcher, S. Pandey, Langmuir 20 (2004) 33.
[21] S.E. Friberg, Q. Yin, F. Pavel, R.A. Mackay, J.D. Holbrey, K.R. Seddon, P.A. Aikens, J. Disper. Sci. Technol. 21 (2000) 185.
[22] Y. Gao, N. Li, L.Q. Zheng, X.Y. Zhao, S.H. Zhang, B.X. Han, W.G. Hou, G.Z. Li, Green Chem. 8 (2006) 43.
[23] S. Creighton, J. Hwang, A. Warshel, W. Parson, J. Norris, Biochemistry 27 (1988) 774.
[24] W. Kuhlbrandt, Nature 374 (1995) 497.
[25] A.H. Herz, Adv. Colloid Interface Sci. 8 (1977) 237.
[26] M. Gouterman, in: D. Dolphin (Ed.), The Porphyrins, Academic Press, New York, 1979, pp. 1–165.
[27] P. Borsenberger, A. Chowdry, D. Hoesterey, W. Mey, J. Appl. Phys. 44 (1978) 5555.
[28] A. Waggoner, J. Membr. Biol. 27 (1976) 317.
[29] E. Hanamura, Phys. Rev. B 37 (1988) 1273.
[30] F. Sasaki, S. Kobayashi, Appl. Phys. Lett. 63 (1993) 2887.
[31] Y. Wang, Chem. Phys. Lett. 126 (1986) 209.
[32] Y. Wang, J. Opt. Soc. Am. B 8 (1991) 981.
[33] S. Kobayashi, Mol. Cryst. Liq. Cryst. 217 (1992) 77.
[34] P. Schouten, J. Warman, M. De Haas, M. Fox, H. Pan, Nature 353 (1991) 736.
[35] J.P. Collman, J.T. McDeevitt, G.T. Yee, C.R. Leidner, L.G. McCullough, W.A. Little, J.B. Torrance, Proc. Natl. Acad. Sci. U.S.A. 83 (1986) 44581.
[36] R. Bonnett, Chem. Soc. Rev. (1995) 19.
[37] M. Kobayashi, H. Tajiri, T. Hayashi, M. Kuroki, I. Sakata, Cancer Lett. 137 (1999) 83.
[38] I.E. Borissevitch, S.C. Gandini, J. Photochem. Photobiol. B: Biol. 43 (1998) 112.
[39] R.F. Pasternack, E.J. Gibbs, A. Antebi, S. Bassner, L. Depoy, D.H. Turner, A. Williams, F. Laplace, M.H. Lansard, C. Merienne, M. Perrée-Fauvet, J. Am. Chem. Soc. 107 (1985) 8179.
[40] J.M. Ribó, J. Crusats, J.A. Farrera, M.L. Valero, J. Chem. Soc., Chem. Commun. (1994) 681.
[41] N.C. Maiti, M. Ravikanth, S. Mazumdar, N. Periasamy, J. Chem. Phys. 99 (1995) 17192.
[42] E.D. Sternberg, D. Dolphin, C. Bruckner, Tetrahedron 54 (1998) 4151.
[43] R.F. Pasternack, E.J. Gibbs, in: A. Siegel, H. Siegel (Eds.), Metal Ion in Biological Systems, Marcel Dekker, 1996.
[44] M. Urbanova, V. Setnicka, V. Kral, K. Volka, Biopolymers 60 (2001) 307.
[45] S.M. Andrade, S.M.B. Costa, Biophys. J. 82 (2002) 1607.
[46] S.M. Andrade, S.M.B. Costa, J. Fluoresc. 12 (2002) 77.
[47] R.F. Pasternack, E.J. Gibbs, P.J. Collings, J.C. depaula, L.C. Turzo, A. Terracina, J. Am. Chem. Soc. 120 (1998) 5873.
[48] A.S.R. Koti, N. Periasamy, Chem. Mater. 15 (2003) 369.
[49] K. Behera, P. Dahiya, S. Pandey, J. Colloid Interface Sci. 307 (2007) 235.
[50] K. Behera, M.D. Pandey, M. Porel, S. Pandey, J. Chem. Phys. 127 (2007) 184501.
[51] K. Behera, S. Pandey, J. Colloid Interface Sci. 316 (2007) 803.
[52] K. Behera, S. Pandey, J. Phys. Chem. B 111 (2007) 13307.
[53] K. Behera, S. Pandey, Langmuir 24 (2008) 6462.
[54] K. Behera, S. Pandey, J. Colloid Interface Sci. 331 (2009) 196.
[55] K. Behera, H. Om, S. Pandey, J. Phys. Chem. B 113 (2009) 786.
[56] A. Sarkar, M. Ali, G.A. Aker, S. Tetin, Q. Ruan, S. Pandey, J. Phys. Chem. B 113 (2009) 3088.
[57] A. Sarkar, S. Trivedi, G.A. Baker, S. Pandey, J. Phys. Chem. B 112 (2008) 14927.
[58] A. Sarkar, S. Trivedi, S. Pandey, J. Phys. Chem. B 112 (2008) 9042.
[59] M. Ali, A. Sarkar, M. Tariq, A. Ali, S. Pandey, Green Chem. 9 (2007) 1252.
[60] M. Ali, A. Sarkar, M.D. Pandey, S. Pandey, Anal. Sci. 22 (2006) 1051.
[61] M. Ali, G.A. Baker, S. Pandey, Chem. Lett. 37 (2008) 26.
[62] K. Kalyanasundaram, Photochemistry of polypyridines and porphyrin complexes, Academic Press, New York, 1991.
[63] D.L. Akins, in: T. Kobayashi (Ed.), J-aggregates, World Scientific, Singapore, 1996.
[64] N.C. Maiti, S. Mazumdar, N. Periasamy, J. Porphyr. Phthalocyan. 2 (1998) 369.
[65] A.S.R. Koti, N. Periasamy, J. Mater. Chem. 12 (2002) 2312.
[66] I.E. Borissevitch, T.T. Tominaga, H. Imasato, M. Tabak, J. Lumin. 69 (1996) 65.
[67] J. Wu, N. Li, K. Li, F. Liu, J. Phys. Chem. B 112 (2008) 8134.

[68] D. Frolov, S. Bagdonas, L. Kelbauskas, W. Dietel, G. Streckyte, R. Rotomskis, Lithuanian J. Phys. 41 (2001) 484.
[69] R.F. Pasternack, C. Fleming, S. Herring, P.J. Collings, J. Depaula, G. Decastro, J.E. Gibbs, Biophys. J. 79 (2000) 550.
[70] D.L. Akins, H.R. Zhu, C. Guo, J. Phys. Chem. 100 (1996) 5420.
[71] D.L. Akins, H.R. Zhu, C. Guo, J. Phys. Chem. 98 (1994) 3612.
[72] N.C. Maiti, S. Mazumdar, N. Periasamy, J. Phys. Chem. B 102 (1998) 1528.
[73] D.L. Akins, H.R. Zhu, C. Guo, J. Phys. Chem. B 105 (2001) 1543.
[74] P.G. Van Patten, A.P. Shreve, R.J. Donohoe, J. Phys. Chem. B 104 (2001) 5986.
[75] X. Yang, Z. Dai, A. Miura, N. Tamai, Chem. Phys. Lett. 334 (2001) 257.